Preferred citation: C.P.J. Bennington and J.P. Mmbaga. Liquid-Phase Turbulence in Pulp Fibre Suspensions. In **The science of papermaking**, *Trans. of the XIIth Fund. Res. Symp. Oxford, 2001*, (C.F. Baker, ed.), pp 255–286, FRC, Manchester, 2018. DOI: 10.15376/frc.2001.1.255.

LIQUID-PHASE TURBULENCE IN PULP FIBRE SUSPENSIONS

C.P.J. Bennington and J.P. Mmbaga

Department of Chemical and Biological Engineering, and
Pulp and Paper Research Institute of Canada
Pulp and Paper Centre, The University of British Columbia,
Vancouver, BC, Canada V6T 1Z4

ABSTRACT

Mixing-sensitive chemical reactions have been used to study liquid-phase turbulence in a number of dispersed two-phase systems, including pulp fibre suspensions. This technique has allowed the measurement and mapping of turbulence in a number of mixing configurations at pulp mass concentrations up to $C_m = 0.10$ (expressed as a fraction). Liquid-phase turbulence was found to decrease exponentially with suspension concentration, indicating that fibres are extremely efficient at dampening turbulence within a suspension. The magnitude of turbulence reduction correlates well with the reduction in gas-liquid mass transfer, an indirect measure of liquid-phase turbulence. The energy dissipated by the fibre network is compared to predictions made using fibre network theory.

INTRODUCTION

The generation of motion in pulp fibre suspensions is essential in all aspects of pulp and paper processing. Pumping, mixing and paper forming operations all apply energy to disrupt the fibre suspension at the floc and/or fibre level. With the input of sufficient energy a fully dispersed state can be

attained, although a flocculated state is rapidly re-established once energy dissipation ceases.

The interrelationships between energy input, turbulence and flocculation have been studied for pulp suspensions in a number of fibre systems, primarily for suspensions at low mass concentrations ($C_m < 0.01$). Direct measurement of turbulence in these systems is difficult due to the opacity of the suspensions and/or the invasive nature of the measurement techniques used. Most tests have shown that fibres reduce suspension turbulence.

The modification of turbulence in non-fibrous particulate flows has been extensively studied. Of the mechanisms known to modify turbulence, two predominant ones are the dissipation of power from an eddy due to the acceleration of particles, and disturbances of the flow due to the wake and vortices shed by the particles. Interaction between particles is governed by a number of factors. Gore and Crowe [1] related turbulence modification to the size of the particles. They found that small particles (relative to the length scale associated with the most energetic eddies in the suspending fluid phase) reduced turbulence, while large particles increased it. The demarcation between enhancement and suppression occurred at $d_p/l_e = 0.1$ where d_p was the particle diameter and l_e the size of the most energetic eddy. Hetsroni [2] included the effects of fluid viscosity and relative density in his examination of literature data, using the particle Reynolds number to characterize turbulence. Particles having $Re_p < 110$ tended to suppress turbulence while those having $Re_p > 400$ tended to increase turbulence. In the latter case, this was attributed to vortices shed by the particles. Particles were also found to change the energy spectra. Both an increase and decrease in the high frequency spectral components were reported. Most experimental data were obtained at low particulate loading with spherical particles in either pipe or free-jet flows. While these studies offer insight into interactions between a dispersed and fluid phase, they do not fully represent the interactions occurring in a pulp fibre suspension.

A number of studies have examined turbulence in pulp and model fibre suspensions. These have employed a range of measurement techniques, including impact probes, laser doppler velocimetry (LDV), optical attenuation, photographic methods, and the use of conductive, thermal and dyed tracers [3]. Some tests with pulp suspensions have been made at mass concentrations as high as $C_m = 0.06$, although most were limited to lower concentrations (typically $C_m < 0.01$) because of the experimental technique used. Interference between fibres and invasive probes and attenuation of optical signals due to suspension opacity were common limitations cited.

Pulp fibres were found to generally attenuate turbulence although turbulence enhancement was also observed. Kerekes and Garner [4] measured tur-

bulence intensity in channel flow of a $C_m = 0.005$ pulp suspension using LDV. The average turbulence intensity was reduced by 11 to 28% when compared with water, although an increase in turbulence at higher frequencies (scales less than 2 mm) was also reported. This was interpreted as the inability of the LDV to distinguish between fibres and the seeded fluid phase. Steen [5] used nylon fibres and a refractive index matching technique to measure turbulence in vertical pipe flow at mass concentrations up to $C_m = 0.012$ using LDV. At low concentrations, short fibres (1 mm) increased turbulence at scales comparable with the fibre length. Longer fibres (3 mm) and higher mass concentrations decreased turbulence at all scales. The reduction in turbulence was attributed to formation of a fibre network. More recently, refractive index matching has been used to measure turbulence in glass fibre suspensions up to $C_m = 0.20$ [6] where fully turbulent suspension flow was found to resemble single-phase flow with respect to both mean and RMS velocity fluctuations.

Turbulence measurements made using other experimental techniques have found similar results to the LDV findings described above [3]. While most work has concluded that fibres dampen turbulence, exceptions to this were found. This is perhaps to be expected due to the difficulty measuring turbulence in two-phase systems even at low suspension concentrations, and the complex interactions that occur between fibres, fibre flocs and the flow.

In 1988 we began using mixing-sensitive chemical reactions (widely applied to aqueous systems, see Baldyga and Bourne, 1999 [7]) to probe mixing and turbulence within pulp fibre suspensions. The technique can be employed in a manner that is minimally invasive, and has now yielded mixing and liquid-phase turbulence measurements for pulp suspensions at mass concentrations as high as $C_m = 0.10$. Here, we detail the experimental procedures used to apply these reactions in pulp fibre suspensions. This technique has allowed quantification of liquid-phase turbulence and mapping of energy dissipation in a number of mixing devices. Our results are compared with tests made in aqueous systems, and with tests made in other dispersed systems (including synthetic fibre suspensions and bead dispersions). Finally, the energy dissipated by the fibre network is compared to predictions made using established fibre network theory.

EXPERIMENTAL

Mixing-sensitive chemical reactions

Certain chemical reactions are mixing-sensitive and can be used to study mixing. These are typically rapid, competitive-consecutive or parallel reaction systems. By controlling reaction chemistry, the distribution of the

reaction products can be used to define the degree of mixing occurring in a system. Qualitative assessment can be made using the product distribution alone. Quantitative assessment can be made using suitable mathematical models to link reaction kinetics with mixing hydrodynamics. Using this procedure it is possible to determine the turbulent energy dissipation experienced by the reaction.

Several mixing-sensitive reaction schemes have been developed by Baldyga and Bourne [7] and used to study mixing systems. The azo coupling between 1-naphthol (A_1) and diazotized sulfanilic acid (B) is a classic example of a competitive-consecutive reaction. The reaction scheme can be written as [8]

$$A_1 + B \xrightarrow{k_{1o}} o\text{–}R \tag{1}$$

$$A_1 + B \xrightarrow{k_{1p}} p\text{–}R \tag{2}$$

$$o\text{–}R \xrightarrow{k_{2p}} S \tag{3}$$

$$p\text{–}R \xrightarrow{k_{2o}} S \tag{4}$$

where o–R and p–R are mono-substituted dye stuffs and S is the bis-substituted dye stuff. Dye concentrations are determined spectroscopically using linear regression techniques once reaction is complete.

Experiments are normally conducted in a semi-batch mode, with B maintained as the limiting reagent and added slowly to one location in the mixer. Micromixing experiments are made by ensuring that the feed time of B, t_f, is long compared to a critical feed time, t_c, which marks the point at which macroscale effects begin to influence reaction. The critical feed time is readily determined experimentally and must be measured for each mixer configuration.

The relative yields of the dyes are given by product distributions based on the limiting agent used (B). For the competitive-consecutive reaction described above (Equations 1–4) as

$$X_S = \frac{2c_S}{c_{o\text{–}R} + c_{p\text{–}R} + 2c_S} = \frac{2c_S}{c_R + 2c_S} \tag{5}$$

The isomers of R are difficult to separate spectroscopically and their sum is used to compute the product distribution [9,10]. Performing a mass balance on the limiting reagent B can be used to check the accuracy of a test.

The reaction rates, k_{1o}, k_{1p}, k_{2o}, k_{2p}, are given by Bourne et al. [8]. The

competitive-consecutive reaction scheme allows mixing assessment in systems with energy dissipation up to 200–400 W/kg. By adding 2-naphthol (A_2) to the system ($k_3 > k_{2o}$) the range of accessible energy dissipation is increased to 10^5 W/kg. Here

$$A_2 + B \xrightarrow{k_3} Q \tag{6}$$

with competition occurring between A_1 and A_2 for B. Two product distributions can be evaluated

$$X'_S = \frac{2c_S}{c_{o-R} + c_{p-R} + c_Q + 2c_S} \tag{7}$$

and

$$X_Q = \frac{2c_Q}{c_{o-R} + c_{p-R} + c_Q + 2c_S} = \frac{c_Q}{c_R + c_Q + 2c_S} \tag{8}$$

with X_Q being used to quantify mixing at higher energy dissipation levels. Here little S is formed and reaction proceeds as a parallel reaction system.

Quantifying mixing

The product distributions can be used directly for qualitative assessment of mixing. As the intensity of mixing increases, the quantity of dye produced by the slower reaction is reduced. For example, both X_S and X_Q decrease with increasing mixing intensity. However, the product distribution may not vary significantly over all energy dissipation ranges. The reaction chemistry and test conditions must be chosen based on the anticipated energy dissipation in the mixer.

Quantitative assessment of the local mixing intensity requires the use of mathematical models that combine mixing with the reaction kinetics. Many models are available [7], and we have used the engulfment model developed by Baldyga and Bourne [11] for our analyses. This model can be used when diffusion does not influence reaction rate (i.e. when $Sc \ll 4000$ and $c_B^o \gg c_A^o$. With B maintained as the limiting reagent, the product distribution X_Q depends on:

$$X_Q = f\left(kinetics, \frac{N_{A1}^o}{N_B^o}, \frac{N_{A2}^o}{N_{A1}^o}, Da, \frac{V_A}{V_B}\right) \tag{9}$$

Once the reaction conditions are fixed (which we do by choosing a mixer, selecting reaction concentrations, volumetric ratios and the operating temperature) the product distributions depend only on the Damköhler number, which is the ratio of the time for micromixing to the time for chemical reaction

$$Da = \frac{k_{2o} c_B^o}{E(1 + V_A/V_B)} \tag{10}$$

Da is related to the turbulent energy dissipation through the engulfment rate coefficient, *E*

$$E = 0.058\sqrt{\varepsilon/v} \tag{11}$$

By comparing experimentally measured product distributions with those computed for the test conditions using the engulfment model [7,11], the local mixing intensity, *e*, can be determined as illustrated in Figure 1.

The accuracy of mixing assessment depends upon test reproducibility and the accuracy with which the product dyes can be measured. In an aqueous system, replicate tests showed that X_S could be determined to within ± 0.005 [12] and X_Q to ± 0.003 [10]. The experimental accuracy can be evaluated by comparing the total moles of dye produced, $(V_A + V_B)(c_Q + c_{o-R} + c_{p-R} + 2c_S)$, with the quantity of limiting reagent used in a test, $(V_B c_{Bo})$. For tests made in aqueous solution, mass balances were found to be typically $98.2 \pm 1.3\%$ (standard deviation) [13].

Dealing with dye adsorption on a solid phase

When a solid phase is present during reaction the product dyes can adsorb onto it. The total extent of adsorption can be estimated by using the mass balance described above. If one product dye is preferentially adsorbed, the measured product distribution will change independently of the energy dissipated during reaction. Consequently, adsorption must be accounted for to correctly assess mixing and energy dissipation in a system.

Pulp fibres adsorb the dyes produced during the azo coupling reactions described above. Fortunately there are several methods that can be used to

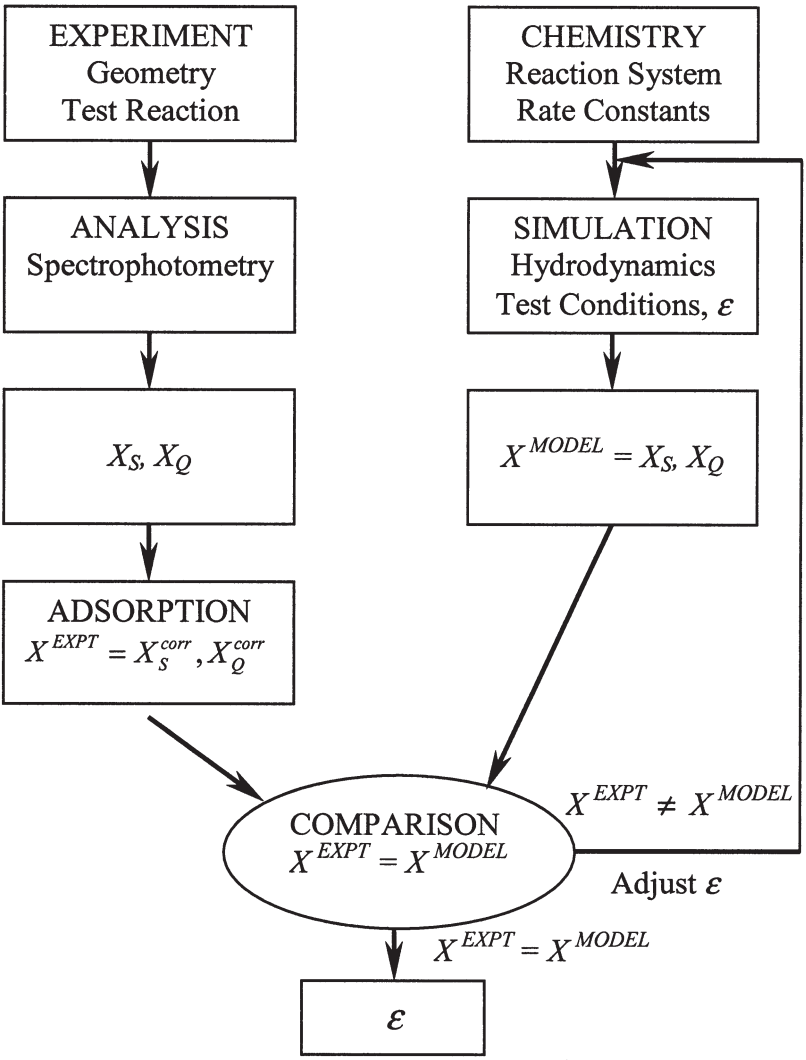

Figure 1 Scheme for evaluating local energy dissipation based on mixing-sensitive tests and mathematical models linking mixing and chemical reaction.

prevent or correct for adsorption allowing the reaction techniques to be applied in dispersed systems.

The first method is to treat the fibres so that they no longer adsorb the dyes. We found that repeatedly dyeing fibres saturated the adsorption sites so that further adsorption did not occur during a test [12]. The repeated dyeing was time consuming and could only be used when small quantities of fibre were needed. Fibre physical properties were also modified slightly by the repeated suspension handling, although this was not characterized.

Using a model fibre suspension that does not adsorb the dyes circumvents the adsorption problem. Indeed, model suspensions are often used as surrogates for pulp suspensions. The limitation is that model suspensions do not behave identically to pulp suspensions, which can complicate interpretation of the results.

Finally, dye adsorption onto a given pulp fibre can be characterized. This allows the product distribution measured in a suspension to be corrected for adsorption prior to data analysis and interpretation [10,14]. For example, for one FBK fibre tested, the following equation was developed to correct the product distribution for adsorption [10]

$$X_Q^{corr} = \frac{X_Q^{meas}}{1.0 - 8.62C_m + 47.33C_m{}^2} \tag{12}$$

where X_Q^{meas} is the product distribution measured following the test and X_Q^{corr} is the product distribution corrected for adsorption.

The tests required to develop these correlations are time consuming and apply only for the particular fibre type and chemical conditions used. The need to correct the product distribution increases the error for any given measurement and care must be taken to ensure that complete dye adsorption does not occur. Often the use of a particular material must be restricted to an upper limit of suspension concentration due to the extent of dye adsorption. For example, tests with nylon fibre suspensions were restricted to $C_m < 0.05$. Once a correlation has been developed for a given fibre it can be used directly in micro-mixing tests.

Test apparatus used

Mixing-sensitive chemical reactions can be used in any mixer or apparatus provided that full macroscale mixing is achieved in the device. This is needed to ensure that the limiting reagent reacts in an A-rich environment and is fully consumed during the test. Under these conditions the measured product

distribution can be accurately related to the local energy dissipation in the mixer.

Four mixing devices were used in the tests described here. Low-consistency pulp suspensions ($C_m < 0.03$) were studied using two conventional stirred-tank reactors (STs) agitated with Rushton turbines. For $C_m > 0.03$, suspensions were studied in medium- and high-intensity mixers to ensure that the full vessel contents were mixed. Diagrams of the mixers are given in Figure 2, with dimensional details provided in Table 1.

Temperature was controlled for all tests. In ST_2 and the medium-intensity mixer, constant temperature water baths were used to control temperature. For the high-intensity mixer, multiple injection points minimized the time

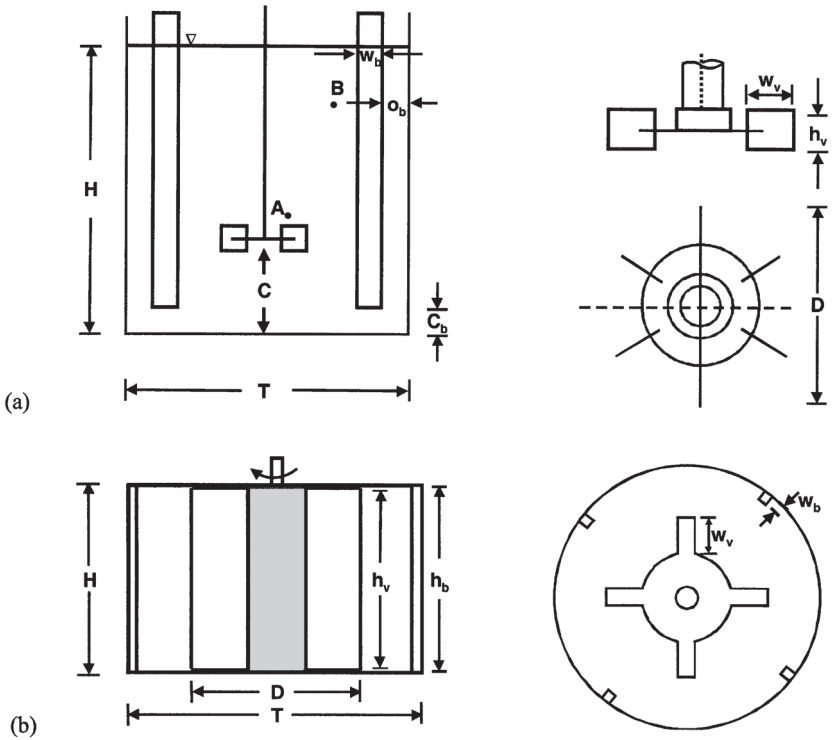

Figure 2 Mixing devices used in tests. (a) Stirred tank reactors with Rushton turbines; (b) medium- and high-intensity mixers. Mixer dimensions given in Table 1.

Table 1 Dimensions of mixing devices studied

Parameter (dimensions in mm)	Mixer			
	ST_1	ST_2	Medium-Intensity Mixer	High-Intensity Mixer
Vessel				
T	150	300	190	220
H	150	300	100	100
Baffles				
n_b	4	4	4	6
h_b	150	300	100	100
w_b	13	26	10	10
c_b	13	26	0	0
o_b	15	30	0	0
Impeller/Rotor				
D	50	100	100	100
n_v	6	6	4	6
h_v	10	20	100	100
w_v	13	26	25	25
C	50	100	0	0
Net Operating Volume, L	2.5	21.2	2.5	3.4
Attached Power, W	~37	250	250	22500
Max. Avg. Power Dissipation, W/kg	14.8	11.8	100	6620

required for chemical injection while flow through a cooling circuit controlled temperature.

Test procedure

Chemical conditions for each test were based on previous work and could be determined using the anticipated energy dissipation in conjunction with micromixing models. For tests conducted in the medium-intensity mixer, the following chemical conditions were used: $c^o_{A1} = 0.52$ mol/m^3, $c^o_{A2}/c^o_{A1} = 2.0$ and $c^o_B = 21.54$ mol/m^3 with $N^o_{A1}/N^o_B = 1.2$ and $V_A/V_B = 50$ [13]. In all cases, B was maintained as the limiting reagent. The required concentration and volumes of naphthols were prepared and added to a known fibre mass to give a suspension having target mass and chemical concentrations. Just prior to a

test, the naphthol mixture was buffered to $pH = 9.9$ using Na_2CO_3 and $NaHCO_3$, giving a solution having an ionic strength of 444.4 mol/m^3. The suspension was thoroughly mixed and allowed to equilibrate for 20 minutes prior to a test.

Tests were conducted in a semi-batch manner. Freshly prepared diazotized sulfanilic acid (*B*) was metered gravimetrically at the selected feed-point location using a constant-flow micro-pump (Ismatec, Switzerland). The feed-rate was set so that the solution feed-time was greater than the critical feed-time, which was determined experimentally. All reactions were conducted at $T = 25 \pm 0.5$°C.

Following complete addition of *B*, a sample of the aqueous phase was taken, diluted with buffer solution, and analyzed spectrophotometrically (UV-Visible Diode Array Spectrophotometer, HP5284A, Hewlett Packard, Waldbronn, Germany) for the product dyes.

Reaction takes place in a limited region within the vessel as shown in Figure 3. Here the reaction volume was visualized in an aqueous system using an acid-base neutralization and a suitable pH-sensitive indicator. Note that the reaction zone fluctuated significantly over short time intervals (on the order of milliseconds). The product distribution measured in any test is determined by the integrated energy dissipation experienced in the small reaction volume over the test period.

To correctly interpret the average local energy dissipation during a test, reaction must be conducted under micromixing controlled flow conditions. Results for a typical test series in which the feed-time of *B*, t_f, was varied is given in Figure 4. All other test conditions (chemical and physical) were fixed. The product distribution, here X_S, decreased as the feed-rate of *B* was reduced (feed-time lengthened). The point at which an asymptotic value of X_S was attained is called the critical feed-time, t_c. If *B* is added to the mixer faster than *A* can be transported there by circulation within the vessel, a stoichiometric imbalance occurs and the reaction no longer takes place in an *A*-rich environment. Consequently, the secondary reaction increases and the product distribution is no longer governed solely by the local energy dissipation. While this can be modeled, it complicates analysis and requires that bulk flow within the vessel be known. For $t_f > t_c$ reaction is governed only by the local energy dissipation, a condition used in all the analyses that follow.

The critical feed-time must be measured experimentally. To avoid measuring t_c for every test condition, it was measured under conditions where the slowest macromixing occurred. This was at the lowest impeller speeds, and for fibre suspensions, at the highest mass concentration. By measuring t_c

under these conditions, and ensuring that $t_f > t_c$ for all subsequent tests (made at higher N or lower C_m), we know that the feed-time of B will not affect the product distribution.

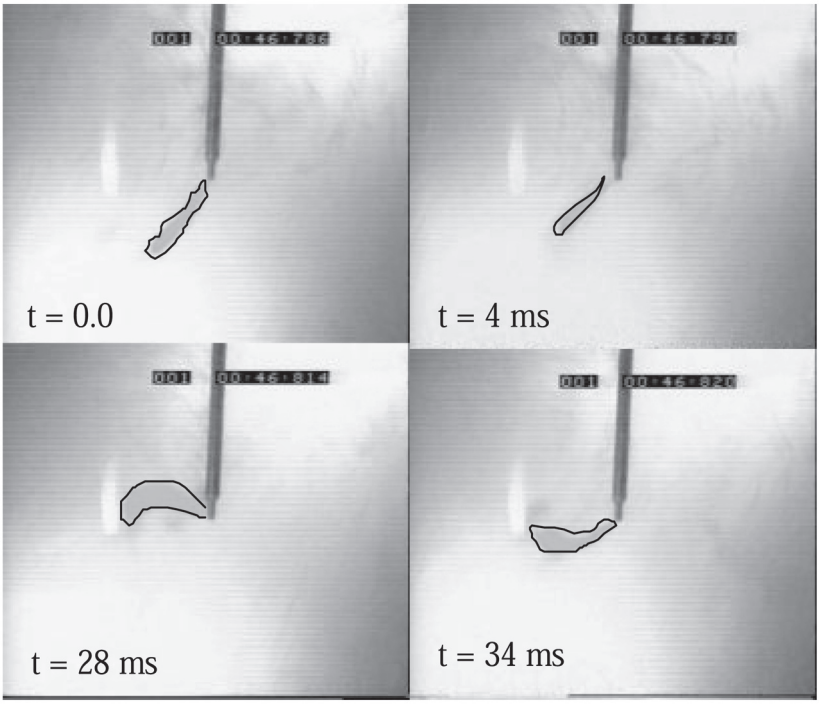

Figure 3 Sequential images show the variability in both the location and volume of the reaction zone in the medium-intensity mixer with time (the elapsed time is given in each image). Feedpoint F_{33}, $N = 7.3$ rev/s. The neutralization reaction between the basic (darker) feed stream was observed during mixing into an acidic solution under similar flow conditions used in the azo coupling tests. Phenolphthalein was used as the indicator. The reaction zone is intensified for ease of identification in the images.

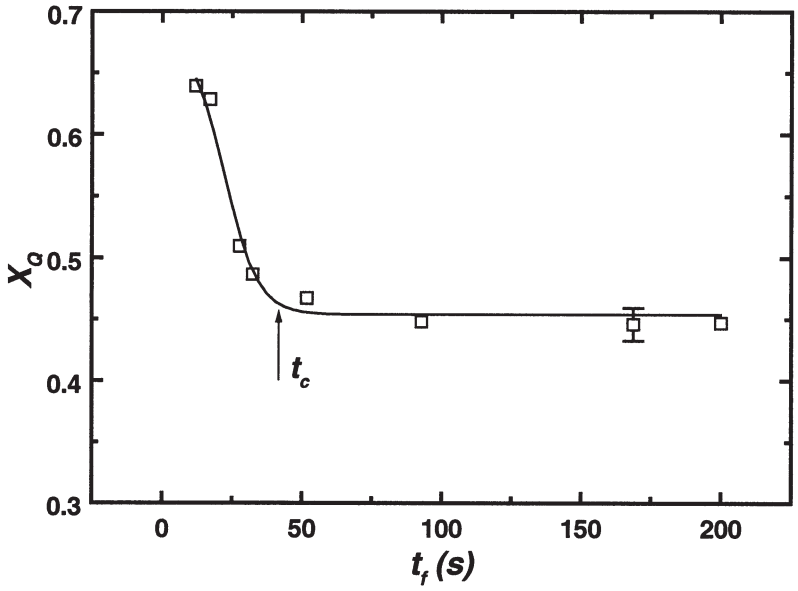

Figure 4 Production distribution versus B feed-time for a typical micromixing test showing determination of the critical feed-time.

RESULTS AND DISCUSSION

Confirmation of test procedures using water

Tests were made in aqueous systems to act as reference cases against which the effect of the fibre suspensions could be compared. Water tests were also used to ensure that the micromixing model accurately predicted the test conditions. For example, Figure 5 plots the product distribution against impeller speed for the azo-coupling reaction conducted at two different locations in ST_1 [12]. For water agitated by a Rushton impeller in this mixer configuration both the flow field and chemical kinetics are known. Using a micromixing model that includes the convective transport of reactants through the different energy dissipation zones in the vessel allows the product distribution to be calculated at different feed locations over a range of impeller speeds. The agreement between the experimental data and model is good. In situations where the flow field is not known, the average local energy dissipation can be estimated using the procedure illustrated in Figure 1.

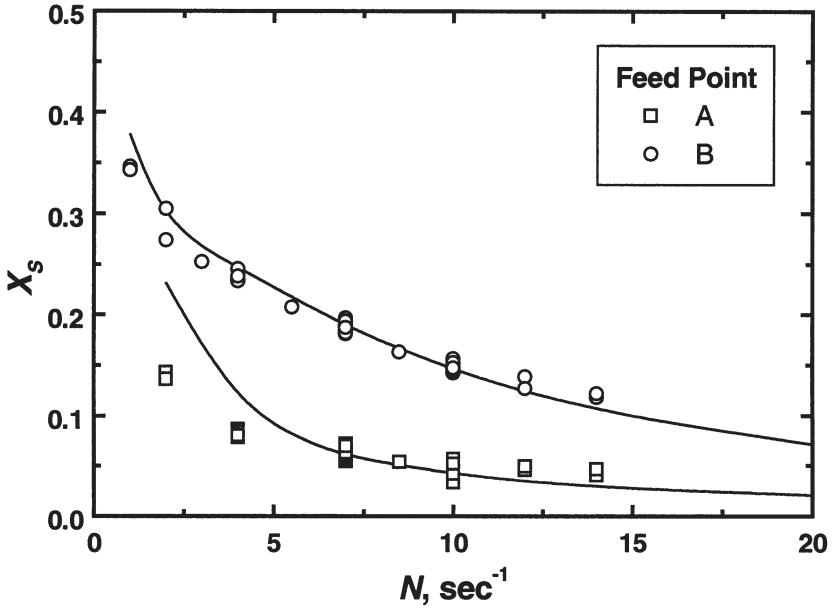

Figure 5 The agreement between experimental tests and modeled predictions for the coupling of 1-naphthol with sulfanilic acid in ST_1. Semi-batch operation at $t_f > t_c$. $c^o_{A1} = 0.52$ mol/m^3, $V_A/V_B = 50$, $N^o_A/N^o_B = 1.1$. Feed-point A is in the suction flow immediately above the impeller, Feed-point B is away from the impeller near the top of the mixer [12].

Mixing low-consistency pulp suspensions in a stirred tank reactor

The pulp suspension must be in complete motion throughout the vessel for a test to be conducted in the microscale regime. Consequently, the shear stress imposed by the impeller must exceed the yield stress of the suspension everywhere in the mixer. This is difficult to achieve in regions remote from the impeller, and becomes more difficult as the suspension mass concentration increases. For example, in ST_2 at $C_m = 0.025$, complete suspension motion was not obtained until an impeller speed of $N = 12$ s^{-1} was reached.

Micro-mixing tests were conducted in ST_2 at two feed-points using kraft pulp suspensions [14]. For the feed-point at the top of the mixer (away from the impeller) and at any impeller speed, the product distribution (corrected for dye adsorption) increased as suspension mass concentration increased. This indicates a reduction in local energy dissipation. Figure 6 plots the

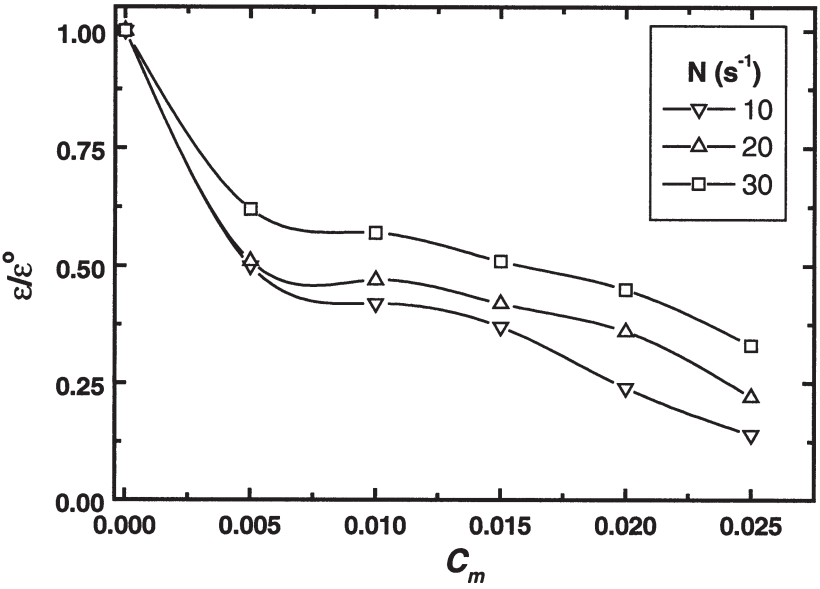

Figure 6 Relative liquid-phase power dissipation in ST_2 as a function of pulp suspension mass concentration and impeller speed. Feed location B.

relative energy dissipation (water is used as the reference) against the suspension mass concentration. Each curve shows a significant reduction in energy. Even at mass concentrations as low as $C_m = 0.005$ energy dissipation in the liquid phase could be reduced up to 50%. Similar results were found at a second feed point located in the intake flow to the impeller.

In all but one test the input impeller power for the pulp suspension was higher than or equal to the power used in the corresponding water case. For this single case, conducted at the feed location near the impeller and at $N = 14$ s^{-1}, the relative power dissipation increased at $C_m = 0.005$. This measured increase reflects a decrease in ε^o attributed to the formation of a vortex in the water case. The vortex did not form in the pulp suspensions.

The reduction in relative power dissipation differed between feed-points and depended on the impeller speed and suspension concentration. This indicated that the spatial distribution of energy dissipation changed as mixing and suspension conditions changed. It was not possible to determine the extent of the energy redistribution as only two feed locations were measured.

The reduction in local energy dissipation was attributed to energy expended in continually disrupting the fibre-fibre contacts in the suspension network. An attempt to explain the reduction using the apparent viscosity of the suspension was not satisfactory [14].

Mixing in the medium- and high-intensity mixers

The yield stress of a pulp fibre suspension increases markedly with mass concentration, typically as the 2.3–3.6th power [15]. As suspension mass concentration rises, it becomes extremely difficult to create fluid-like flow throughout any vessel. Typically stagnant regions form at a distance from the impeller where the applied shear stress falls below the suspension yield stress. This gives a cavern of active motion whose size depends on both the suspension rheology and power input. Maintaining a 'fluid-like' state, particularly at medium mass concentrations ($0.08 \leq C_m \leq 0.14$), requires continued dissipation of significant energy. Estimates for the power required to 'fluidize' a $C_m = 0.10$ suspension range from 850 to 14,000 W/kg (based on a suspension density of 1000 kg/m^3) [16,17]. The medium- and high-intensity mixers used in this study (Figure 2) achieve this under specific operating conditions. In essence, they represent mixing devices in which the bulk circulation zone has all but been eliminated, leaving only the high intensity impeller zone.

Suspension rheology is best characterized by the volumetric concentration, C_v. This also facilitates comparison between different types of fibres and other particulate systems. For a pulp fibre suspension, C_v is calculated knowing the mass concentration of fibre, C_m, the amount of water adsorbed in the fibre wall leading to fibre swelling, X_w, the volume of the fibre lumen, V_L, and a measure of the amount of gas present in the suspension. This latter quantity can be determined if the bulk density of the suspension is known. For a typical kraft fibre suspension having $X_w = 1.2$ kg/kg where the fibres are fully collapsed ($V_L = 0$) and there is no gas in the suspension, $C_v \approx 2C_m$.

Comparison between different suspensions is best made using volumetric concentrations. For example, the $C_m = 0.20$ glass fibre suspension used by Andersson in his LDV studies has a volumetric concentration of $C_v = 0.08$. A $C_m = 0.061$ FBK suspension (with $X_w = 0.62$) has the same volumetric concentration.

Figure 7 plots X_Q^{corr} versus the impeller speed for tests made in water and with low consistency FBK suspensions in the medium-intensity mixer. For water, X_Q decreases as N increases. This indicates increasing energy dissipation with increased energy input, as expected. This same trend is observed for the fibre suspensions except that the curves were shifted to higher values of X_Q^{corr} despite the fact that the power input to the system remained the same.

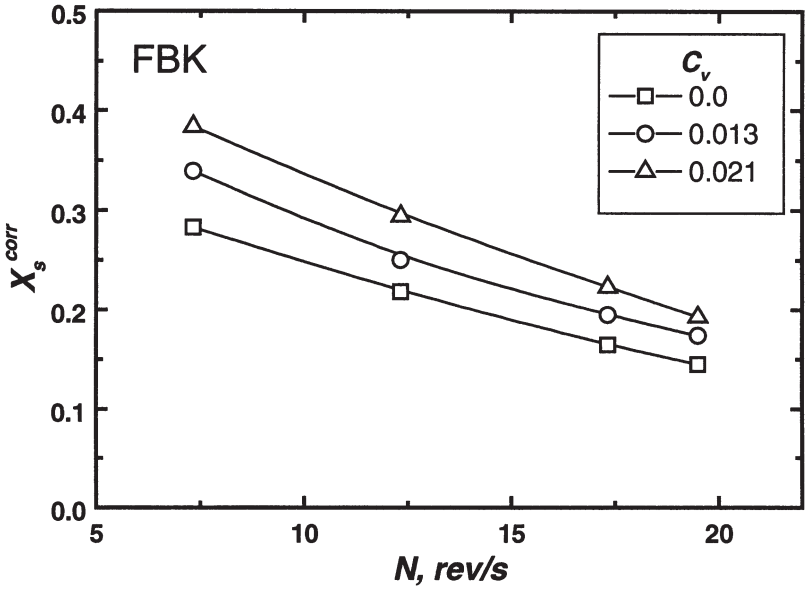

Figure 7 X_Q^{corr} versus impeller speed for FBK suspensions at $C_m = 0.00 - 0.016$ ($C_v = 0.0 - 0.021$). Medium-Intensity mixer at feed point F_{32} (see Figure 10). $c_{A2}^o/c_{A1}^o = 2$, $V_A/V_B = 50$, $c_{A1}^o = 0.52$ mol/m^3, $c_B^o = 21.54$ mol/m^3, $t_f = 180$ s, $T = 25$°C.

The ability of different suspensions to attenuate liquid-phase turbulence is given in Figure 8. Here the relative energy dissipation ($\varepsilon/\varepsilon^o$) is plotted as a function of suspension volume concentration for FBK, and for two polyethylene fibre suspensions. The fibres are characterized by their aspect ratio, A, and the beads by their diameter ($d_p = 2.7$ mm). Tests were run in the medium-intensity mixer at $N = 7.3 - 19.5$ s^{-1} under identical reaction conditions.

The spherical beads attenuated liquid-phase turbulence, in agreement with the literature findings [1,18,19]. Attenuation is increased for the polyethylene fibre suspensions, with the extent of attenuation increasing with fibre aspect ratio. The FBK fibre suspension ($A = 105$) attenuated turbulence to the same extent as the lower aspect ratio polyethylene fibres ($A = 84$). While a number of reasons might contribute to this difference (fibre stiffness, fibre density, etc.), the most likely reason is the different fibre-length distribution between the two fibre types. The polyethylene fibres were more monodisperse, with most fibres falling between 3.0 and 4.0 mm in length. The pulp fibres, on the

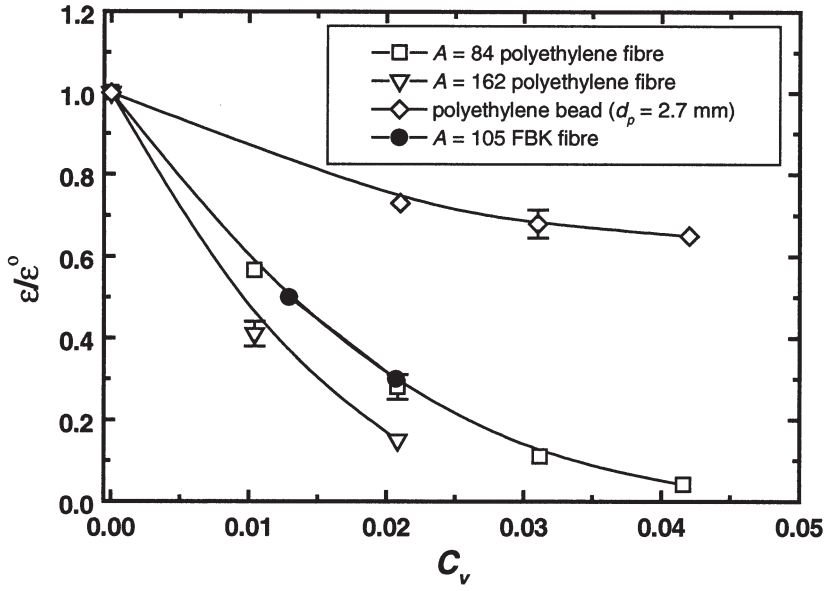

Figure 8 Relative liquid-phase energy dissipation versus volumetric concentration for fibres of different aspect ratios and for a suspension of polyethylene beads. Tests made in the medium-intensity mixer at feed point F_{32} over a range of impeller speeds ($N = 7.3 - 19.5$ s^{-1}) using the reaction conditions given in Figure 7.

other hand, spanned a wide range, from 0.25 to 4.5 mm, with most fibres falling below 0.5 mm in length. Our use of the length weighted fibre-length to calculate A (which has been found to relate well with measured pulp sheet properties and was 2.3 mm for the FBK pulp tested) heavily weighted the longer fibres in the suspension. As most fibres are much smaller than this average length, they do not contribute to turbulence modification to the same extent as the larger fibres. Consequently the higher aspect ratio pulp fibres attenuated turbulence as readily as the lower aspect ratio polyethylene fibres.

The relative energy dissipation is plotted versus the volumetric concentration in Figure 9 for tests made using FBK suspensions in the high-intensity mixer between $N = 50$ and 83.3 s^{-1}. The data can be correlated with the volumetric concentration of the suspension using

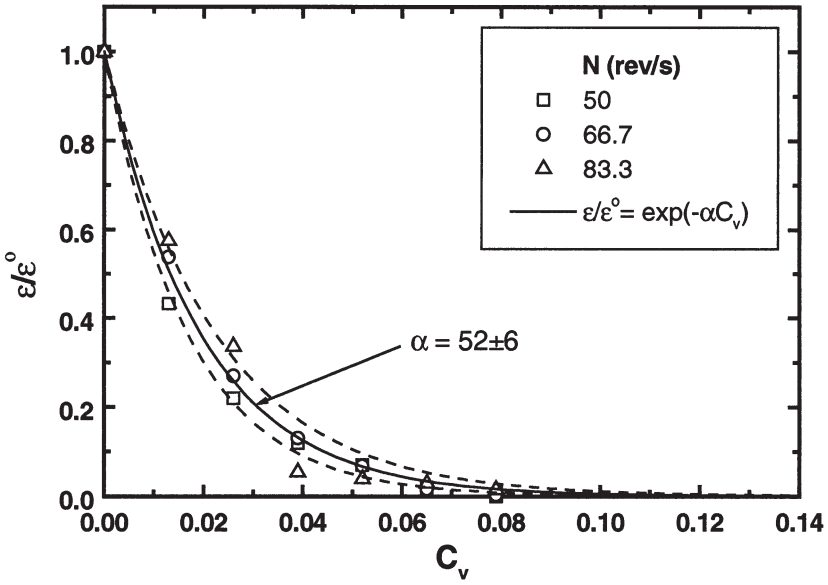

Figure 9 Relative liquid-phase energy dissipation versus volumetric concentration for FBK suspensions in the high-intensity mixer at three impeller speeds. The solid line is the fit of the data to an exponential decay function using the volume concentration.

$$\frac{\varepsilon}{\varepsilon^o} = \exp(-\alpha C_v) \tag{13}$$

where α is the liquid-phase turbulence attenuation factor. For the FBK suspension, α was found to be 52 ± 6 at the 95% confidence interval.

Our studies with other dispersed systems showed that liquid-phase turbulence was also affected by particle density and size [13]. Studies with glass beads showed that for $d_p > 0.55$ mm turbulence was reduced at all concentrations while for the smallest particles ($d_p = 0.11$ mm) turbulence was enhanced slightly. These findings are similar to those reported by Villermaux et al. [20] and Barresi [21]. They also agree with the analysis of Buyevich [22] with regard to energy dissipation due to particle collisions.

The density of the particulate material also affected turbulence dissipation. The glass bead dampened turbulence more effectively than polyethylene bead of nearly equivalent size. Again, these observations concur with information previously reported in the literature [2,18,19].

For fibre suspensions, the critical factor affecting energy dissipation is the ability of the suspension to form a network. Thus, it is expected that the fibre aspect ratio and volumetric concentration should dominate energy dissipation, as demonstrated by the experiments. Other fibre factors are also expected to influence energy dissipation and include fibre flexibility and density, although they have not been investigated.

Mapping spatial energy dissipation in suspensions

The local energy dissipation within a mixer can be mapped by conducting tests at feed-points located throughout the region of interest. The accuracy of the resulting energy-dissipation map depends on the number of tests used in preparing it, and a compromise must be made between the accuracy required and the time available to conduct measurements. To map just one plane within the medium-intensity mixer we used fifteen test points, arranged as shown in Figure 10. The local bulk flow and energy dissipation can vary at

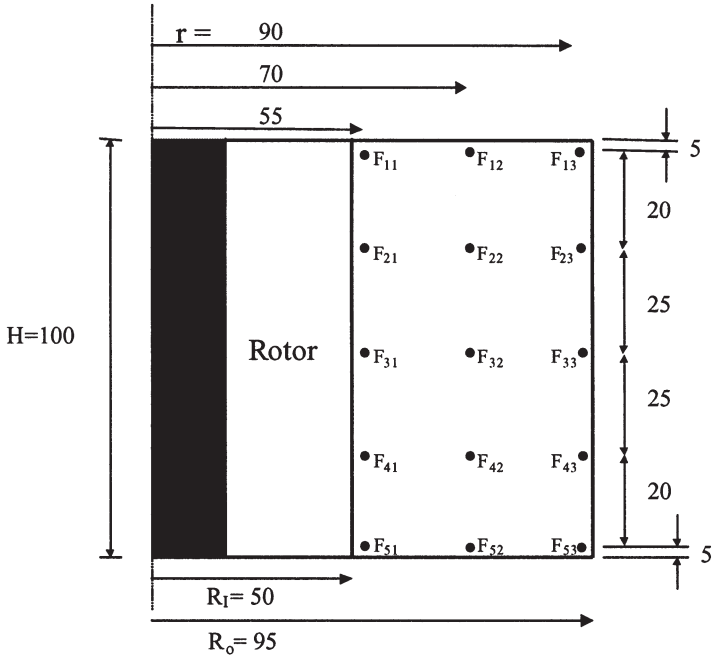

Figure 10 Cross-section of mixing vessel showing feed-point locations for 2D profile measurements. Dimensions in millimeters.

each feed location, which results in changes in the volume and location of each reaction zone throughout the mixer. This can be observed in aqueous systems (as shown previously in Figure 3) but cannot be seen in opaque suspensions. In the analysis that follows, the feed-points were fixed at the exit of the feed-pipes and the Kriging method used to interpolate between data points.

Figure 11 plots the dimensionless energy dissipation, $\phi = \varepsilon_i/\varepsilon_{avg}$, in the sample plane for tests made with water and with a $C_m = 0.017$ FBK suspension. Tests were conducted under identical chemical reaction conditions at an impeller speed of $N = 17.3$ rev/s. The average energy input to the system was similar in both cases (101 ± 6 W/kg for water and 100 ± 6 W/kg for the FBK suspension).

The average energy dissipation in the liquid phase, ε_{avg}, was calculated by averaging the individually measured local dissipation values and weighting

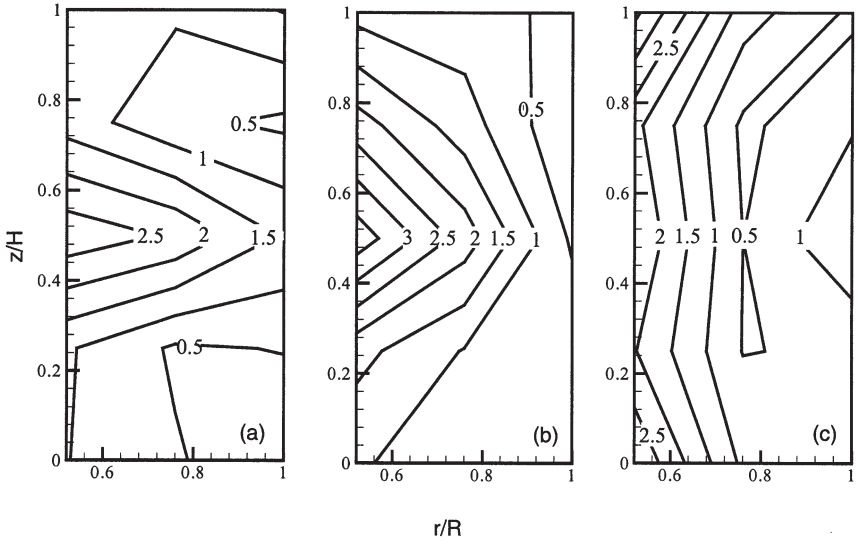

Figure 11 Two-dimensional dimensionless energy dissipation map in a plane midway between wall baffles for (a) water ($\varepsilon_{in} = 101 \pm 5$ W/kg, $\varepsilon_{avg} = 120 \pm 13$ W/kg); (b) a $C_v = 0.0215$ FBK suspension ($\varepsilon_{in} = 101 \pm 5$ W/kg, $\varepsilon_{avg} = 33 \pm 5$ W/kg); (c) and a gas-water dispersion ($\phi_g = 0.20$) ($\varepsilon_{in} = 67 \pm 4$ W/kg, $\varepsilon_{avg} = 71 \pm 8$ W/kg). Test conditions: $c^o_{A1} = 0.52$ mol/m^3, $c^o_{A2}/c^o_{A1} = 2.0$ and $c^o_B = 21.54$ mol/m^3 with $N^o_{A1}/N^o_B = 1.2$ and $V_A/V_B = 50$.

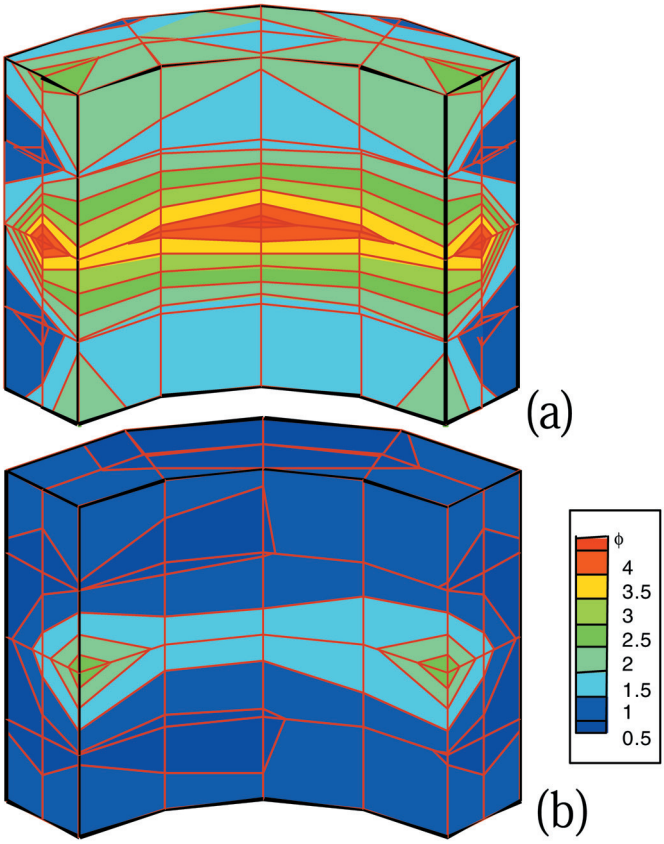

Figure 12 Three-dimensional dimensionless energy dissipation map for (a) water and (b) a $C_v = 0.021$ polyethylene fibre suspension in the medium-intensity mixer at $N = 17.3\ s^{-1}$ as observed from the impeller tips. Test conditions as in Figure 11. (Water: $\varepsilon_{in} = 101 \pm 5$ W/kg, $\varepsilon_{avg} = 106 \pm 10$ W/kg); Polyethylene suspension: $\varepsilon_{in} = 104 \pm 6$ W/kg, $\varepsilon_{avg} = 41 \pm 6$ W/kg). ε_{avg} based on 85 points.

them according to the volume fraction of mixer they represent. For the water case, the calculated average energy dissipation using the mixing-sensitive chemical reactions was 120 ± 13 W/kg, in agreement with the measured power input. For the FBK suspension, the average energy dissipation in the liquid phase was reduced by 67% (to 33 ± 5 W/kg). This reduction in liquid-phase turbulence was of similar magnitude to results obtained using a single point measurement (F_{32}), indicating that a thoughtfully chosen feed point can be used to gauge overall suspension behaviour.

For both the water and pulp suspension tests the bulk flow within the vessel was similar. Flow left the impeller radially outwards at its centre, and returned to the impeller at the top and bottom of the vessel. The energy dissipation profiles were also similar. The most intense energy dissipation occurred in the impeller vicinity and was highest in the discharge flow. However, for pulp suspensions, the peak relative energy dissipation was slightly higher than for water and the gradient in change of energy dissipation steeper. When gas (nitrogen) was added to the suspension (Figure 11(c)) the energy dissipation profile flattened out somewhat and became more uniform throughout the vessel ($\varepsilon_{in} = 67 \pm 4$ W/kg, $\varepsilon_{avg} = 71 \pm 8$ W/kg).

A three-dimensional map of the medium-intensity mixer was made for water and for a $C_v = 0.021$ suspension of polyethylene fibre ($A = 85$). Due to geometrical similarity, only one-quarter of the mixer volume was mapped. Even so, the five planes measured in the quarter-volume required a total of 85 tests. As shown in Figure 12, the energy dissipation for the fibre suspension was more uniform than for the equivalent water case. This is contrary to the finding for the FBK suspension based on the single plane test shown in Figure 11(b).

We also measured the energy dissipation between the vanes of the rotor (a further 15 tests). In this case, for water, we find that $\varepsilon_{avg} = 115 \pm 10$ W/kg compared with an ε_{in} of 101 ± 6 W/kg. For the polyethylene fibre suspension liquid-phase energy dissipation was reduced by 51% (ε_{in} of 104 ± 6 W/kg, $\varepsilon_{avg} = 51 \pm 6$ W/kg).

Parallels with gas-liquid mass transfer

Gas-liquid mass transfer was measured in an FBK fibre suspension of varying mass concentration in a laboratory mixer similar to the high-intensity mixer. The sulfite oxidation technique was used to measure the volumetric gas-liquid mass transfer coefficient, $k_L a$ [23]. Fitting the relative change in $k_L a$ to an exponential decay function, as had been done for the liquid-phase turbulence, gave

$$\frac{k_L a}{k_L a^o} = \exp(-50 C_v) \tag{14}$$

(The decay function had a 95% confidence interval of ±13). The decay coefficients for liquid-phase turbulence dampening (α in Equation 13) and for reduction in gas-liquid mass transfer were the same within experimental error. This indicates that the reduction in gas-liquid mass transfer was correlated with and may be due to the reduction in liquid-phase turbulence caused by the fibres.

Modeling turbulence suppression in pulp fibre suspensions

When energy dissipation is measured using mixing-sensitive chemical reactions, only energy dissipated in the fluid phase is measured. As shown above, this energy can be significantly less than the input energy, even for suspensions of low mass concentration.

Energy dissipation must occur between components of the suspension. These include fibre-fibre interactions, interactions between the fibre and fluid, and turbulence dissipation within the fluid. Power that does not end up in the liquid phase must be dissipated by fibre-fibre interaction, of which friction at the fibre-fibre contact points is expected to be a large contributor. If we assume that the majority of energy not measured in the liquid phase is dissipated through fibre-fibre friction, then we can write

$$\varepsilon_{in} \cong \varepsilon_{ff} + (1 - C_m - C_m X_w)\varepsilon_{avg} \tag{15}$$

where ε_{in} is the input energy, and ε_{ff} is the energy dissipated through fibre-fibre friction in W/kg of suspension. ε_{avg} is the energy dissipated in the aqueous phase measured using the mixing-sensitive reactions and expressed as W/kg of the liquid phase. This must be adjusted to W/kg of suspension and is accomplished by computing the mass fraction of free water as a function of total suspension mass.

Assuming the idealization of a homogeneous isotropic suspension, we can use a mathematical description of the fibre network to estimate the contribution of fibre-fibre friction to energy dissipation in the suspension. The energy dissipated by fibre-fibre friction per kilogram of suspension can be expressed as

$$\varepsilon_{ff} = \mu_f F_N N_C u_r \tag{16}$$

where μ_f is the coefficient of friction between fibres, F_N the normal force at a

fibre contact point, N_C the number of active fibre-fibre contacts per kilogram of suspension, and u_r the relative velocity at the contact points, which can be taken as the average fluctuating velocity.

The normal force acting at a fibre-fibre contact point can be estimated using beam bending theory [24]. Here

$$F_N = \frac{6\delta EI}{(\Delta l)^3} \tag{17}$$

where δ is the bending deflection which is proportional to the fibre diameter d and is set to $\delta = 0.6d$ [25]. EI is the fibre stiffness and Δl is the distance between contact points on the fibre which can be estimated by dividing the fibre length by the number of contacts per fibre, *i.e.* $\Delta l = l/n_c$.

Expressions for the number of contacts in a homogeneous random network of fibres have been given by a number of investigators. Wahren [26] gives the following equation relating the fibre volume concentration to fibre dimensions and the number of contacts per fibre.

$$C_V = \frac{16\pi A}{\left(\frac{2A}{n_c} + \frac{n_c}{n_c - 1}\right)^3 (n_c - 1)} \tag{18}$$

which can be simplified to

$$n_c = \sqrt{\frac{C_V A^2}{2\pi}} \tag{19}$$

for $1 \ll n_c < A$. n_c is used in calculating the force per fibre contact, as well as determining the total number of distinct fibre contacts per unit mass of suspension, N_c. The latter is given by

$$N_C = N_f n_c^I \tag{20}$$

where N_f is the number of fibres per unit mass of suspension, given by

$$N_f = \frac{C_m}{\omega l} \tag{21}$$

and n_c^I is the number of independent contacts per fibre, which is smaller

than n_c. To estimate n_c^I, we use the crowding factor N_{cr} [27] to calculate the number of fibres in the volume swept out by a single fibre of length l. Here

$$N_{cr} = \frac{2}{3} C_V A^2 \tag{22}$$

The probability that a fibre contact is independent is then given by

$$P_C = \frac{n_c}{N_{cr}} \tag{23}$$

The total number of independent contacts per fibre is thus

$$N_C = N_f n_c^I = N_f P_C n_c = \frac{C_m n_c^2}{\omega l N_{cr}} \tag{24}$$

The fluctuating relative velocity between fibres is not known. However we can estimate u_r by substituting Equations 17 and 24 into Equation 16, using Andersson and Rasmuson's [28] value for μ_f and calculating ε_{ff} using experimental data (the input power minus the measured energy dissipation in the liquid phase). A graphical solution is given in Figure 13 for the FBK fibres in the high-intensity mixer at $N = 66.7$ rev/s with $EI = 3 \times 10^{-12}$ Nm^2 and $X_w = 0.62$. The figure shows that for fibre-fibre friction to attenuate the liquid-phase turbulence that the relative velocity between fibres must decrease rapidly with suspension concentration. At $C_v = 0.026$ ($C_m = 0.02$) Equation 16 would require that $u_r > 20$ m/s for fibre-fibre friction to account for the measured reduction in liquid-phase turbulence. This is unreasonably high as discussed later. When the suspension concentration is increased to $C_v = 0.135$ ($C_m = 0.104$) u_r drops below 2.0 m/s.

There is little information available on the relative movement between fibres in turbulent flow to help us gauge the accuracy of these estimates. Bennington et al. [29] measured average flow velocities for FBK suspensions at $C_m = 0.059$ ($C_v = 0.118$) in the high-intensity mixer at $N = 41.7$ rev/s. Maximum measured velocities were upwards of 4 m/s adjacent to more slowly moving suspension. The technique used (tracing flocs filmed using high-speed cinematography) did not permit fluctuating velocities to be measured. Andersson [6] measured the fluctuating velocity using LDV in a refractive index matched glass-fibre suspension. For a $C_m = 0.10$ ($C_v \cong 0.04$) suspension the RMS velocity was 2 m/s at $N = 42$ rev/s, a point above the onset of fully

turbulent flow. Measured RMS velocities were typically 0.1 to 0.2 times the impeller tip velocity, and depended on the flow regime.

Extending the trend in RMS velocity versus tip speed measured by Andersson allows us to estimate the RMS velocity for the experimental conditions used in Figure 13. This gives u_r values from 2 to 4 m/s. Thus, while fibre-fibre friction can account for attenuation of liquid-phase turbulence at high suspension concentrations (above approximately $C_v = 0.08$), it would seem to require unreasonably high values of the relative velocity at the lower suspension concentrations. However, referring to Figure 8 we see that polyethylene beads, that do not form networks, attenuate turbulence significantly in this range. Likely a combination of mechanisms is at work in fibre suspensions, with fibre-fibre friction becoming significant at higher suspension concentrations.

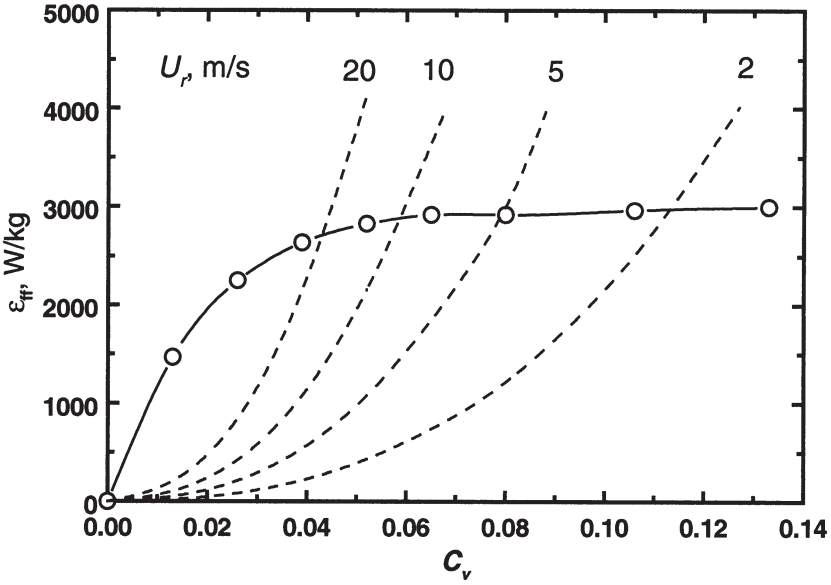

Figure 13 Measured energy dissipation in the fibre-phase (solid line) versus that attributed to fibre-fibre friction (dashed lines) using Equation 16. Data obtained in the high-intensity mixer with FBK at $N = 66.7$ rev/s. Wahren's [26] equation was used to estimate n_c.

SUMMARY AND CONCLUSIONS

Mixing-sensitive chemical reactions can be used to assess the local liquid-phase energy dissipation in pulp fibre (and other dispersed systems) provided that adsorption of the product dyes on the dispersed phase is accounted for. The number of tests required depends on the extent and type of information desired. Single point tests are useful and are readily made. Three-dimensional mapping of energy dissipation of a volume requires extensive testing and can be time consuming.

Tests made on a variety of suspensions showed that liquid-phase turbulence was readily dampened by the dispersed phase. Results made with beads followed the behaviour reported in the literature, with the extent of dampening dependent on suspension concentration, particle size and density. For fibre suspensions, the formation of an inter-connected network further reduced liquid-phase turbulence, particularly at suspension concentrations above $C_v = 0.08$. A simple model of fibre-fibre interaction based on fibre network theory gave a framework for understanding the contribution of fibre-fibre friction to removal of energy from the suspension. The reduction in liquid-phase turbulence as a function of suspension mass concentration was identical to that found for gas-liquid mass transfer in a similar system.

REFERENCES

1. Gore, R.A. and Crowe, C.T., "Effect of Particle Size on Modulating Turbulent Intensity," *Int. J. Multiphase Flow*, 15: 279–289 (1989).
2. Hetsroni, G., "Particles-Turbulence Interaction," *Int. J. Multiphase Flow*, **15**(5): 735–746 (1989).
3. Bennington, C.P.J. and Mmbaga, J.P., "The Use of Mixing-Sensitive Chemical Reactions for the Study of Mixing in Pulp Fibre Suspensions" in "*Mixed-Flow Hydrodynamics*, Advances in Engineering Fluid Mechanics Series," N.P. Cheremisinoff (ed.), Gulf Publishing Co., Houston, TX: pp. 395–420 (1996).
4. Kerekes, R.J. and Garner, R.G., "Measurement of Turbulence in Pulp Suspensions by Laser Anemometry," *CPPA Tech. Sec. Trans*. **8**(3): TR53–TR59 (1982).
5. Steen, M., "On Turbulent Structure in Vertical Pipe Flow of Fiber Suspensions," *Nordic Pulp Pap. Res. J*., **4**(4): 244–252 (1989).
6. Andersson, S.R., "Network Disruption and Turbulence in Fibre Suspensions," PhD thesis, Chalmers University of Technology, Goteborg, Sweden (1998).
7. Balgyga, J. and Bourne, J.R., *Turbulent Mixing and Chemical Reactions*, John Wiley and Sons, Chichester, UK (1999).

8. Bourne, J.R., Kut, O.M. and Lenzner, J., "An Improved Reaction System to Investigate Micromixing in High-Intensity Mixers," *Ind. Eng. Chem. Res*. **31**: 949–958 (1992).
9. Bourne, J.R., Kut, O.M., Lenzner, J. and Maire, H., "Kinetics of Azo Coupling Reactions between 1-naphthol and Diazotized Sulfanilic Acid," *Ind. Eng. Chem. Res.*, **29**: 1761–1768 (1990).
10. Mmbaga, J.P. and Bennington, C.P.J., "The Use of Mixing-Sensitive Chemical Reactions to Study Mixing in Dispersed Fibre Systems: Adsorption of Reactant and Product Dyes on the Dispersed Phase," *Can. J. Chem. Eng.*, **76**(3): 670–679 (1998).
11. Balgyga, J. and Bourne, J.R., "Simplification of Micromixing Calculations: I. Derivation and Application of New Model," *Chem. Eng. J.*, **42**: 83–92 (1989).
12. Bennington, C.P.J. and Bourne, J.R., "Effect of Suspended Fibres on Macro-Mixing and Micro-Mixing in a Stirred Tank Reactor," *Chem. Eng. Comm.*, **92**: 183–197 (1990).
13. Mmbaga, J.P., "The Use of Mixing-Sensitive Chemical Reactions to Characterize Mixing in the Liquid Phase of Fibre Suspensions," PhD thesis, The University of British Columbia (1999).
14. Bennington, C.P.J. and Thangavel, V.K., "The Use of a Mixing-Sensitive Chemical Reaction for the Study of Pulp Fibre Suspension Mixing," *Can. J. Chem. Eng.*, **71**: 667–675 (1993).
15. Bennington, C.P.J., Kerekes, R.J. and Bourne, J.R., "The Yield Stress of Fibre Suspensions," *Can. J. Chem. Eng.*, **68**: 748–757 (1990).
16. Gullichsen, J. and Harkonen, E., "Medium Consistency Technology. I. Fundamental Data," *Tappi*, **64**(6): 69–72 (1981).
17. Bennington, C.P.J. and Kerekes, R.J., "Power Requirements for Pulp Suspension Fluidization," *Tappi J.*, **79**(2): 253–258 (1996).
18. Parthasarathy, R.N. and Faeth, G.M., "Turbulence Modulation in Homogeneous Dilute Particle-Laden Flows," *J. Fluid Mech.*, **220**: 485–514 (1990).
19. Yarin, L.P. and Hetsroni, G., "Turbulence Intensity in Dilute Two-Phase Flows. 3. Effect of Particle Size Distribution on the Turbulence of Carrier Fluid," *Int. J. Multiphase Flow*, **20**(1): 27–44 (1994).
20. Villermaux J., Falk, L. and Fournier, M.C., "Potential Use of New Parallel Reaction System to Characterize Micromixing in Stirred Reactors," *AIChE Symposium Series*, No. 299, Vol. 90: 50–54 (1994).
21. Barresi, A.A., "Experimental Investigation of Interaction between Turbulent Liquid Flow and Solid Particles and its Effects on Fast Reactions," *Chem. Eng. Sci.*, **52**(50): 807–814 (1997).
22. Buyevich, Y.A., "Fluid Dynamics of Coarse Dispersions," *Chem. Eng. Sci.*, **49**(8): 1217–1228 (1994).
23. Rewatkar, V.B. and Bennington, C.P.J., "Gas-Liquid Mass Transfer in Low and Medium Consistency Pulp Suspensions," CSChE Conference, Saskatoon, SK: October 3–6, 1999.
24. Timoskenko, S. and Young, D.H., *Elements of Strengths of Materials*, 5th Edition, Van Nostrand, New York, NY (1968).

25. Farnood, R, Loewen, S. and Dodson, C.T.J., "Estimation of Intra-Floc Forces," *Appita J.*, **47**(5): 391–396 (1994).
26. Wahren, D., "Fibre Network Structures in Paper Making Operations," In *Proceedings of the Conference Paper Science and Technology, The Cutting Edge*, Institute of Paper Chemistry, Appleton, WI: 112–132 (1980).
27. Kerekes, R.J. and Schell, C., "Characterization of Fibre Flocculation Regimes by Crowding Factor," *J. Pulp Pap. Sci.*, **18**(1): 32–38 (1992).
28. Andersson, S.R. and Rasmuson, A., "Dry and Wet Friction of Single Pulp and Synthetic Fibres," *J. Pulp Paper Sci.*, **23**(1):5–11 (1997).
29. Bennington, C.P.J., Kerekes, R.J. and Grace, J.R., "Motion of Pulp Fibre Suspensions in Rotary Devices," *Can. J. Chem. Eng.*, **69**: 251–258 (1991).

NOMENCLATURE

A	fibre aspect ratio l_w/d
c_b	baffle clearance from base of mixing vessel, m
c_i	concentration of i^{th} specie, kmol/m^3
C	impeller clearance from base of vessel, m
C_m	mass concentration, fraction
C_v	volumetric concentration, fraction
d, d_p	fibre or particle diameter, m
D	impeller diameter, m
Da	Damkohler number
E	engulfment rate coefficient, s^{-1}
EI	fibre stiffness, Nm^2
F_N	normal force at fibre contact
h_b	baffle height, m
h_v	vane height, m
H	tank/mixer height or fluid level in mixer, m
k_i	rate constant for production of i^{th} component, m^3/kmol.s
k_La	volumetric gas-liquid mass transfer coefficient, s^{-1}
l	fibre length, m
l_e	size of most energetic eddy, m
l_w	length weighted fibre length, m
n_b	number of baffles
n_c	number of contacts per fibre
n_c^I	number of independent contacts per fibre
n_v	number of vanes on the impeller
N	impeller rotation speed, s^{-1}
N_{cr}	crowding factor (number of fibres in the volume swept out by a single fibre)

N_i moles of component *i*, kmol
N_C number of active fibre-fibre contacts per unit mass of fibre, kg^{-1}
N_f number of fibres per unit mass of fibre
o_b baffle offset from the wall, m
P_C probability of a fibre contact being independent
Re_p particle Reynolds number
Sc Schmidt number
t_c critical feed time, s
t_f feed time, s
T tank/mixer diameter, m
T reaction temperature, °C
u_r velocity at contact points, m/s
V_i volume of i^{th} component in solution, m^3
V_L lumen volume, m^3
w_b baffle width, m
w_i weighting factor for energy dissipation at point *i*, where $\sum_{i=1}^{n} w_i = 1$
w_v vane width, m
X_Q product distribution of mono-azo dye formed with 2-naphthol
X_S, X_S' product distribution of bis-azo dye
X_w water responsible for fibre swelling, kg water/kg fibre

Greek

α attenuation coefficient
δ fibre deflection, m
ε energy dissipation, W/kg
ε_{avg} average energy dissipation, $\varepsilon_{avg} = \sum_{i=1}^{n} w_i \varepsilon_i$, *W/kg*
ε_{ff} energy dissipated by fibre-fibre friction, W/kg
ε_i energy dissipation measured in the liquid phase at point *i* using mixing-sensitive reactions, W/kg
ε_{in} energy input to the suspension measured using mechanical means, W/kg
ϕ_g gas void fraction
ϕ relative energy dissipation, $\varepsilon/\varepsilon_{avg}$ or $\varepsilon_i/\varepsilon_{avg}$
μ_f coefficient of friction at fibre contact
ν kinematic viscosity, m^2/s
ω fibre coarseness, kg/m

Chemical Abbreviations

A	1- and 2-naphthols
A_1	1-naphthol
A_2	2-naphthol
B	diazotized sulfanilic acid
Q	2-(1,4 sulphophenyl-azo)-2-napthol or its ion in alkaline solution
R	the sum of 2-(1,4 sulphophenyl-azo)-1-napthol (o-R) and 4-(1,4 sulphophenyl-azo)-2-napthol (p-R) or their ions in alkaline solution
S	2,4-(1,4 sulphophenyl-azo)-1-napthol or its ion in alkaline solution

Superscripts

corr	corrected for adsorption
meas	measured in an adsorbing medium before correction
o	initial case

Acronyms

FBK	fully bleached kraft

Transcription of Discussion

LIQUID-PHASE TURBULENCE IN PULP FIBRE SUSPENSIONS

C.P.J. Bennington and J.P. Mmbaga

Pulp and Paper Centre, University of British Columbia

Please note that there is a typographical error in the preprints. In Equations 3 and 4 (Volume 1 Page 258) the diazotized sulfanilic acid, B, is missing from the left hand side of the equations. Could you please pencil in ' + B' for both equations. Their reactions must be second order to be mixing sensitive.

The corrected equations are: $o\text{–}R + B \xrightarrow{k_{2p}} S$ (3)

$$p\text{–}R + B \xrightarrow{k_{2o}} S \quad (4)$$

Vincent Craig Australian National University

When your dye adsorbs to your fibre, it may alter the fibre-fibre interaction and therefore alter the friction between the fibres, therefore locally you may have a different friction than in the bulk. Do you think this could be an important effect?

Chad Bennington

Yes, I imagine it could be. The mixing sensitive reaction technique only measures the energy dissipation in the liquid phase of the suspension. If fibre-fibre friction changes then more or less energy will be measured in the liquid phase. In fact, it has been suggested that we could modify the surface friction of the fibres and conduct the mixing sensitive reaction tests to see how accurately the model (Equation 16, Volume 1, Page 278) would fit the data.

Vincent Craig

Do you have more than one dye system that you could try that may adsorb differently?

Discussion

Chad Bennington

This work follows after twenty years of work by Baldyga and Bourne who figured out the chemistry of the azo coupling, the rate constants for the reactions, and the spectra of the product dyes. For example, I quickly showed a slide giving the absorption spectra of the pure dyes. It probably took a PhD student most of his five years to generate the pure dyes, isolate them, and then determine their spectra. So one is faced with an enormous amount of work to find and develop a suitable reaction system. Also, the system must have appropriate reaction rates so that the rates of mixing generated in your system can be measured. Now there are other well characterized mixing sensitive systems available, but they do not have the combination of attributes needed to work in my system

John Roberts Department of Paper Science, UMIST

The adsorption maxima of these azo dyes are notoriously sensitive to pH. Did you have to take any particular precautions about the pH control?

Chad Bennington

The pH is absolutely controlled in this system because the rate constants have been determined at not only a specific pH but a specific ionic concentration.

John Roberts

So you controlled ionic strength *and* pH?

Chad Bennington

Yes. We developed the correlations for adsorption under identical conditions to those used for the mixing experiments.

Sussan Sandberg SCA Hygiene Products AB

This was very interesting, but what would be good to know is, what is the optimal position, because you spoke about A and B – what would be the best place to add, if you were adding something?

Chad Bennington

In these experiments we used the outcome of the mixing-sensitive reactions to measure the local energy dissipation at locations A and B in one specific

mixer. If you were generating a chemical using a missing sensitive reaction scheme then the best feed location would be chosen based on what product you wanted to form. If you wanted to form only R, you would want to have reaction in a zone of very high energy dissipation so that none of the slower reaction would proceed to a significant extent. However, if you wanted the opposite outcome, then a feed point of less energy dissipation would be chosen. So, from a chemical generation point of view, these are the type of criteria you would use.

Ramin Farnood University of Toronto

Have you studied the effect of fines, and what would be your expectation if you had fines in the suspension?

Chad Bennington

We haven't explicitly studied fines. The pulp that we used was a fully bleached Kraft pulp. We used the whole pulp, which didn't have a lot of fines, but it had a distribution of aspect ratios.